How to cite: *Angew. Chem. Int. Ed.* **2021**, *60*, 21062–21068
International Edition: doi.org/10.1002/anie.202107917
German Edition: doi.org/10.1002/ange.202107917

Supramolecular Chemistry

Fuel-Driven and Enzyme-Regulated Redox-Responsive Supramolecular Hydrogels

*Mehak Jain and Bart Jan Ravoo**

Abstract: *Chemical reaction networks (CRN) embedded in hydrogels can transform responsive materials into complex self-regulating materials that generate feedback to counter the effect of external stimuli. This study presents hydrogels containing the β-cyclodextrin (CD) and ferrocene (Fc) host–guest pair as supramolecular crosslinks where redox-responsive behavior is driven by the enzyme–fuel couples horse radish peroxidase (HRP)–H_2O_2 and glucose oxidase (GOx)–*D*-glucose. The hydrogel can be tuned from a responsive to a self-regulating supramolecular system by varying the concentration of added reduction fuel* D*-glucose. The onset of self-regulating behavior is due to formation of oxidation fuel in the hydrogel by a cofactor intermediate GOx[$FADH_2$]. UV/Vis spectroscopy, rheology, and kinetic modeling were employed to understand the emergence of out-of-equilibrium behavior and reveal the programmable negative feedback response of the hydrogel, including the adaptation of its elastic modulus and its potential as a glucose sensor.*

Introduction

Out-of-equilibrium is a thermodynamic state that defines life.[1] This state is often characterized by net flow of matter or energy.[2] A prime example remains the assembly of tubulins into microtubules which oscillates between an assembled state of growth called "rescue" and an autonomous and rapid disassembly phase called "catastrophe".[2b,3] Microtubule formation is a highly regulated process where tubulin dimers incorporating GTP attach in a head-to-tail fashion and polymerize until there is a scarcity of GTP-tubulins in vicinity or due to stochastic events. This out-of-equilibrium shift is partially assisted by hydrolysis of attached GTP into GDP, resulting in disassembly due to conformational change of the tubulins.[4] Various microtubule-associated proteins as biochemical fuels provide, in combination, positive (growth enhancing) and negative (growth reducing) feedbacks leading to self-regulation of microtubule dynamics in a cell.[5] Similar processes involving self-regulation can be observed in biological phenomena, such as cell division,[6] transcription,[7] and motility,[8] that combine the ability to transform kinetically and catalytically controlled reactions into feedback loops to maintain the integrity of a living organism while constantly interacting with its surroundings.

In synthetic soft matter, the introduction of coupled chemical reaction networks (CRNs), capable of generating non-covalent interactions which initiate reversible chemo-mechanical changes in their immediate environment, while still maintaining a material's structure and strength over time, has gained much interest recently.[1b,9] These CRNs can give rise to dynamic and transient assemblies which are activated by a fuel (inorganic, organic, or biochemical) and differ from responsive materials in carrying the ability to self-regulate structural changes by integrating a self-generated stimulus (positive feedback) or counter stimulus (negative feedback).[9a] A pioneering example of a CRN was provided by Boekhoven et al.[10] who described the addition of dimethyl sulfate as fuel to a low molecular weight gelator based on a tris-carboxylate ester, which formed fibers with regeneration capacity based on the concentration of ester forming fuel in the system. Further, the concept of treadmilling in microtubules was more closely captured by Das et al.[11] where histidine was first used to form a transient self-assembled gel based on formation of ester bonds, which then hydrolyze due to cooperative catalysis by proximal histidine groups in the assembled state, driving the gel into a sol. In a recent example, the concept of fuel-driven regeneration of fibers was advanced to program the strength of an aldehyde saccharide hydrogel with consecutive cycles of fuel addition, catalytically generated from a pre-fuel.[12]

In the design of CRNs, the use of enzymes as biocatalysts is highly interesting due to their specificity, high turnover rates, and control over the reaction kinetics. In a prominent example of a citric-acid-fueled self-assembled dipeptide Fmoc-Leu-Gly-OH hydrogel, the enzyme urease combined with its substrate urea acted as dormant deactivator to the system by initiating disassembly of hydrogel in an increasingly basic environment through production of ammonia as an internal negative feedback.[13] In another elegant approach, a self-erasing ink was created using a charge transfer supramolecular polymer based on a coronene salt and dodecyl methyl viologen, which showed structural changes on addition of glucose oxidase and sodium dithionate as redox fuel.[14] While most CRNs reported so far rely on an exogenous pre-fuel or activator to initiate a delayed feedback in the material,[12,14] examples where a single substrate can provide both stimulus and feedback without any extra

[*] M. Jain, Prof. Dr. B. J. Ravoo
Organic Chemistry Institute and Center for Soft Nanoscience
Westfälische Wilhelms-Universität Münster
Corrensstrasse 36, 48149 Münster (Germany)
E-mail: b.j.ravoo@uni-muenster.de
Supporting information and the ORCID identification number(s) for the author(s) of this article can be found under: https://doi.org/10.1002/anie.202107917.

addition of feedback initiator are still limited. We note that although the extra addition of fuel provides more versatile control and modulation of the transition out-of-equilibrium, the amount of residual waste inside the system after several cycles can lead to a lack of cyclability of the CRN and/or the material. In contrast, a single-substrate-promoted self-regulation requires a more unique and delicate programming to balance the kinetics of activating and deactivating reactions while keeping the waste impurities to a minimum.[9d,11a,15]

Here we present a CRN based on molecular recognition of the β-cyclodextrin (CD) and ferrocene (Fc) host–guest pair, which form transient self-assembled hydrogels in the presence of the redox-enzyme-fuel couple horseradish peroxidase (HRP)/H_2O_2 and glucose oxidase (GOx)/D-glucose. The hydrogels have the unique ability to either remain in a responsive state of equilibrium or transfer into an out-of-equilibrium state depending on the concentration of D-glucose (reduction fuel) added to the hydrogel. Fc has been long known for its redox[16] properties and high binding constants in the order of 4800 M^{-1} to form a noncovalent inclusion complex with the CD host in aqueous solution.[17] Interestingly, the oxidized ferrocenium ion (Fc^+) is highly water soluble and has no affinity to CD. Due to these properties, various redox-responsive, bio-active, self-assembled materials have been designed for applications in adhesives, catalysis, diagnostics, and therapeutic delivery systems.[16,17c,18] Nakahata et al. have shown that the redox response can be used to make self-healing and mechanically actuated motors using host–guest interactions.[19]

Herein, the enzyme couple HRP and GOx are utilized to regulate the redox properties of Fc in the hydrogel. As Fc in the gel is oxidized by HRP and fuel H_2O_2, it is converted into positively charged Fc^+ and detaches out of the hydrophobic cavity of CD, disassembling the gel into sol. However, if the sol is provided with a reducing environment by addition of GOx and fuel D-glucose, it assembles back to a hydrogel, thus transitioning between two equilibrium states of gel and sol depending on the redox state of Fc. Reduction of Fc^+ to Fc with GOx in the presence of catalytic amounts of D-glucose as substrate has been exploited in glucose sensors.[20] However, the use of GOx and HRP in a cascade reaction with Fc has not been reported. The product of the GOx and D-glucose reaction is a biocatalytic intermediate (GOx[$FADH_2$]), which interestingly carries dual reactivity towards Fc^+ to recycle Fc but also towards O_2 to form H_2O_2, which in the presence of HRP acts as an oxidation fuel in the CRN. Thus, the presence of responsive or self-regulating behavior to design a cyclic CRN in the hydrogel relies on unique orchestrated kinetics of enzyme intermediate GOx[$FADH_2$] towards each substrate, which plays a central role in either regenerating oxidation fuel (initiating trigger) or reducing Fc (initiating counter trigger, Scheme 1). In this way, we obtain a self-regulated, fuel-driven redox-responsive supramolecular hydrogel, which can autonomously assemble and disassemble in the presence of two enzymes and D-glucose.

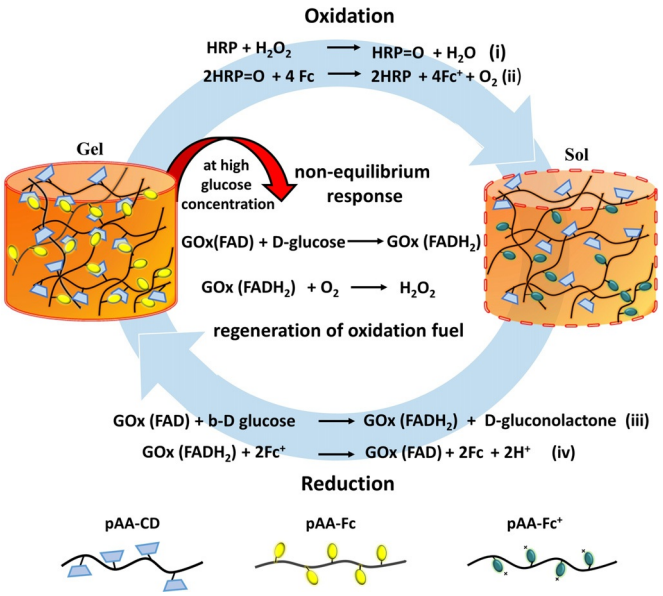

Scheme 1. Fuel-driven redox-responsive hydrogel which can autonomously assemble and disassemble in the presence of D-glucose. The supramolecular hydrogel is comprised of a polyacrylic acid (pAA) backbone with host β-cyclodextrin (CD) and guest ferrocene (Fc) integrated in a noncovalent polymer network. The hydrogel disassembles by addition of enzyme horse radish peroxidase (HRP) and oxidation fuel H_2O_2 by oxidizing Fc into ferrocenium ion (Fc^+). This sol can be transformed back into gel by addition of the enzyme glucose oxidase (GOx) and reduction fuel D-glucose by reducing Fc^+ back to Fc. Up to a threshold concentration of added D-glucose, the hydrogel remains stable, while at higher concentrations the hydrogel shows a non-equilibrium response by autonomously generating oxidation fuel, H_2O_2, for re-oxidation. This negative feedback leads to conversion of gel into sol which can reassemble back into gel by sole addition of D-glucose, since both enzymes remain catalytically active.

Results and Discussion

Fc is an organometallic compound with a low redox potential of +0.403 V [vs. saturated calomel electrode (SCE)],[21] which makes Fc highly sensitive to the redox enzyme couple HRP and GOx.[22] To first analyze the reactivity of redox couple enzymes with Fc, we employed its derivative ferrocene acetic acid owing to its higher solubility in aqueous conditions. 2 mM Fc (in sodium phosphate buffer 0.1 M, pH 7.6) in the presence of (0.1 mM) HRP enzyme and (3 mM) H_2O_2 oxidation fuel at room temperature were oxidized to Fc^+ leading to visible appearance of a deep blue color in the solution which characteristically absorbed at 630 nm (Figure 1 a,b).[16,21,23]

The absorption band is highly sensitive to a change in Fc/Fc^+ oxidation state and hence was used throughout to monitor the redox reaction. Fc^+ was reduced back immediately to Fc by addition of 0.1 mM GOx enzyme and 5 mM D-glucose reduction fuel to the solution, marked by a consistent decrease in absorbance at 630 nm and re-appearance of innate yellow color in the solution (Figure 1 b). Interestingly, the reduced Fc was transiently stable and with time oxidized back to Fc^+ without any further addition of oxidation fuel to the reaction mixture. To understand this better, time-depen-

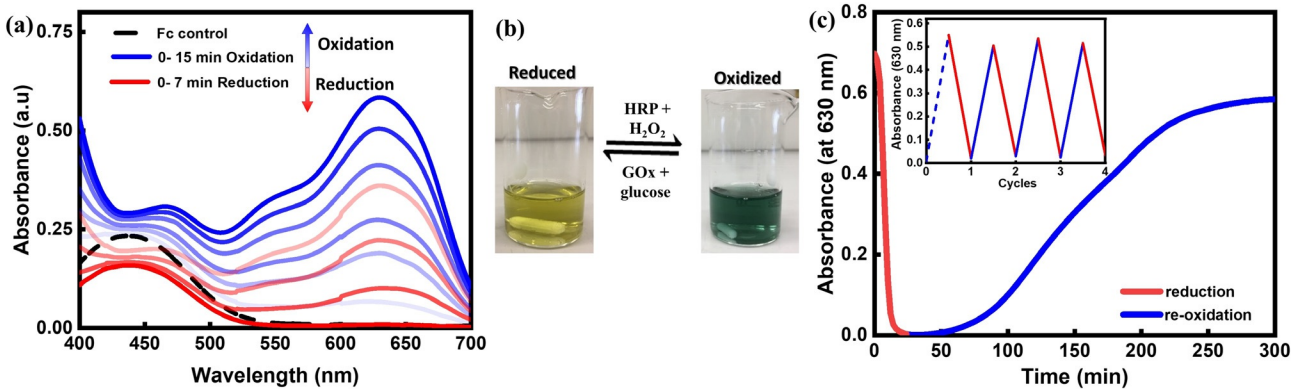

Figure 1. a) UV/Vis spectrophotometric analysis of the redox behavior of ferrocene (Fc) acetic acid in buffer solution at pH 7.6. Initially, Fc had no absorbance at 630 nm, but the 630 nm peak for Fc^+ increased with time (ca. 15 min) as the oxidation fuel H_2O_2 was introduced. After addition of reduction fuel D-glucose to the solution, the absorbance at 630 nm decreased (ca. 7 min). b) A solution of Fc is bright yellow if the reduction fuel and GOx are added and blue for Fc^+ if the oxidation fuel and HRP are added. c) Time-dependent UV/Vis at 630 nm shows the re-oxidation of Fc to Fc^+. Inset shows the final absorbance recorded at the end of each cycle. As the first cycle was fuelled using exogenous H_2O_2 it has been marked with a dotted line. Further cycles required only an addition of D-glucose, regenerating the oxidation fuel autonomously for each cycle.

dent UV/Vis experiments were designed to observe this re-oxidation behavior at the specific wavelength 630 nm. Briefly, into a fresh 2 mM Fc^+ ion solution, containing (0.1 mM) HRP from prior oxidation and no residual H_2O_2, 0.1 mM GOx and 5 mM D-glucose were added and measurement was started without any delay (Figure 1c). We emphasize that control experiments were carried out to make sure there was no residual hydrogen peroxide present from earlier oxidation SI Figure S1, methods (v)(i).

First an immediate reduction to Fc was observed marked by a fast decrease in absorption at 630 nm, followed by a short induction period which showed no change in absorption, and finally a gradual increase in absorption was seen, until it reached saturation. The solution at the end of the measurement visibly consisted of Fc^+. The re-oxidation behavior was tested for 4 more cycles by adding a fixed 5 mM concentration of D-glucose at the end of each cycle (Figure 1c, inset). We note that cascade reactions of GOx and HRP have been used for the modification of soft matter such as fabrication of bio-functional liquid crystal droplets,[24] nanoreactor coacervates,[25] mechanoresponsive sponges,[26] and biocatalytic electrodes.[27] The mechanism of the cascade reaction involves oxidation of D-glucose by GOx largely aided by its cofactor FAD to form β-D-gluconate ions and $FADH_2$. GOx[$FADH_2$] then loses the accepted pair of electrons by reaction with molecular oxygen (O_2) and forms hydrogen peroxide and GOx[FAD]. The H_2O_2 so formed acts as a substrate for HRP for further reactions.[28] In the current CRN the reduced GOx[$FADH_2$] could either react with atmospheric O_2 to form H_2O_2 or with Fc^+ to form Fc and thus oxidize back into its original form GOx[FAD]. To further verify the importance of O_2 for production of H_2O_2 control experiments were performed in cascade with enzymes HRP, GOx and D-glucose for Fc and ABTS. The chromophore substrate 2,2′-azino-bis(3-ethylbenzothiazoline)-6-sulfonic acid (ABTS) and Fc were used to analyze the formation of H_2O_2 in the presence and absence of O_2. ABTS in the presence of H_2O_2 is known to change into the chromophore $ABTS^{\bullet+}$ radical cation, which absorbs at 420 nm while formation of Fc^+ was analyzed at 630 nm as before using UV/Vis spectroscopy.[24,26] While in the presence of O_2, ABTS and Fc converted rapidly into $ABTS^{\bullet+}$ and Fc^+, respectively, on reaction with H_2O_2, there was no transformation seen in either case in the of absence of O_2 (SI Figure S2, methods (v)(ii)). From the above experiments, it appears that GOx[$FADH_2$] reduces Fc^+ ions first, providing Fc instantly, and then reacts with O_2 to form H_2O_2, which in the presence of HRP reformed the oxidation fuel initiating in situ re-oxidation of Fc (Scheme 1). Before transferring these characteristics to a hydrogel, a deeper understanding of the kinetics of the cascade reaction was required to control and modulate the negative feedback (re-oxidation) arising in the CRN.

As can be observed from Figure 1c, the redox reaction can be divided into three major steps: a) oxidation of Fc in the presence of oxidation catalyst HRP and fuel H_2O_2 to form Fc^+, (b) reduction of Fc^+ in the presence of reduction catalyst GOx and fuel D-glucose to from Fc, and (c) generation of H_2O_2 in situ due to atmospheric O_2 leading to negative feedback. Kinetic parameters K_m, V_{max}, and K_{cat} were obtained for each step by carrying out Michaelis–Menten kinetics on the three individual reactions (SI methods (iii)(c), Figure S3, Table S1). By comparing kinetic parameters from the above reactions, it was clear that the V_{max} for reduction of Fc^+ into Fc was significantly higher than for all other reactions thus explaining the observed behavior of GOx to first reduce Fc^+ and only then produce H_2O_2, but considering the fact that the kinetics were carried out on each set independently of each other the possibility of interference between reactions cannot be ruled out. Kinetic models for carrying out computational simulations of in vitro or in vivo enzyme cascade reactions were designed earlier to gain insights into the rate-determining steps,[29] limiting factors for bio-transformations,[30] and optimization of intricate reaction set ups.[31] Simulations were thus carried out by creating a cascade reaction model following Michaelis–Menten kinetics (SI Figure S3, S4, S5). To complement the results of kinetic

modeling studies, time-dependent UV/Vis experiments with varying concentrations of D-glucose to modulate the rate of re-oxidation were also performed (Figure 2). As before, to a fresh solution of 2 mM Fc^+ (with a constant amount (0.1 mM) of HRP from oxidation), a constant amount of 0.1 mM GOx with different amounts of D-glucose (1, 2, 5, 10 and 20 mM) was added to individual experiments. All the studies were done in triplicates with constant conditions for temp, pH, and substrate concentrations.

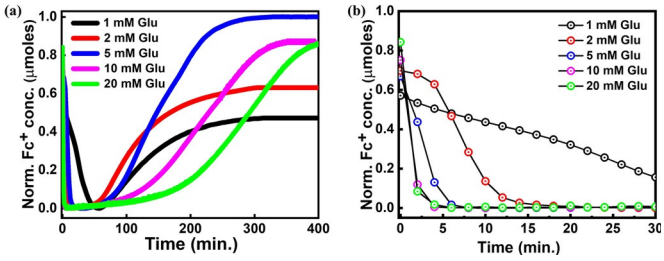

Figure 2. a) Time-dependent UV/Vis measurements conducted at 630 nm (Fc^+) for different concentration of D-glucose. The absorbance data were used to calculate the normalized concentration of Fc^+. b) Reduction of Fc^+ to Fc as observed in the first 30 min of the experiments.

The results from UV/Vis spectroscopy (Figure 2, SI Figure S6) and simulations (SI Figure S5) clearly show that the reduction of Fc^+ was directly proportional to the concentration of D-glucose supplied to the network. Indeed, at 1 mM D-glucose it took nearly 60 min until Fc^+ was completely reduced, whereas for 20 mM D-glucose it took less than 5 min to completely reduce all Fc^+ in the solution (Figure 2b). Also, simulations (SI Figure S5) indicate that the V_{max} for the reaction of GOx[$FADH_2$] with Fc^+ was more than 10 times higher than for the reaction with O_2 (SI Table S1), implying that the reaction would always proceed in a forward direction irrespective of the amount of O_2 present. The higher rate of reduction can likely be attributed to the "ball–funnel" model[32]" derived from the crystal structure of GOx, where $FADH_2$ forms a funnel-shaped cavity and Fc^+ fits into the cavity like a ball, as the positive charge on Fc^+ leads to stronger interaction with the negatively charged $FADH_2$ cofactor in comparison to O_2. Moreover, based on simulations, the induction period[33] between the reduction and beginning of re-oxidation reflects the time period required for GOx[$FADH_2$] to switch its reactivity from Fc^+ to O_2. Only once Fc and H_2O_2 are regenerated in the reaction, the re-oxidation can be re-initiated. These observations suggested that the response and rate of negative feedback in the CRN can be tuned and modulated by tuning the time and amount of H_2O_2 generated in a hydrogel which in turn proposed a linear dependence on the concentration of D-glucose (SI Figure S5).

However, it was experimentally observed that the induction period and the re-oxidation response had a threshold dependence on D-glucose concentration around 5 mM, until which the negative feedback increases (going from 1 mM to 5 mM) but subsequently decreases after crossing the threshold value (at 10 and 20 mM, see Figure 2a). The increase in negative feedback with increased concentration is likely due to a lack of D-glucose at 1 and 2 mM, which implies there was not enough oxidation fuel generated below a D-glucose concentration of around 5 mM at which point the shortest induction period is observed, accompanied by fastest re-oxidation leading to early saturation. On the other hand, the reason for much slower feedback at higher concentration (10 and 20 mM) can be explained by effect of substrate inhibition of GOx in the presence of excess D-glucose.[34] It is also important to note that the product of D-glucose oxidation, D-gluconolactone, slowly hydrolyzes to D-gluconic acid, which has a very similar structure increasing the effect of competitive inhibition along with substrate inhibition.[35]

Encouraged by the analysis of the redox properties of Fc in the presence of enzyme couple, supramolecular hydrogels of pAA-CD and pAA-Fc were prepared using polyacrylic acid (pAA) as polymer backbone.[36] Briefly, 4 wt % solutions of pAA-CD and pAA-Fc were prepared in 0.1 M boric acid KCl buffer at pH 9.0 (SI methods (ii), (vii), Figure S14, S15). Physical mixing of both polymers (CD:Fc) in 1:0.5, 1:1, and 1.25:1 ratios gave the desired gel (pAA-CD/pAA-Fc) with varying storage modulus (G′). For all the experiments pAA-CD:pAA-Fc 1.25:1 with G′ ≈ 100 Pa was used. The hydrogels so formed were stable for more than 30 days. Characteristic rheological parameters such as sheer strain (γ %) and angular velocity (ω rad sec^{-1}) for the pAA-CD/pAA-Fc gels were determined by measuring the linear viscoelastic region (SI Figure S7) and were kept consistent as ($\gamma = 1\%$, $\omega = 1$ rad sec^{-1}) throughout all the rheological measurements. Like many supramolecular gels the pAA-CD/pAA-Fc gel also had the ability to self-heal[37] via molecular recognition (SI Figure S8). To first test the response of the supramolecular hydrogel towards oxidation fuel, HRP (0.3 mM) and minimum required H_2O_2 (0.25 M) were added and the gel was slowly stirred using a 6 mm rice bead stir bar (Figure 3). The change in G′ was measured with time to observe a constant decrease until the gel completely changed into sol.

The time required for the gel to completely disassemble into sol was found to be dependent on the concentration of

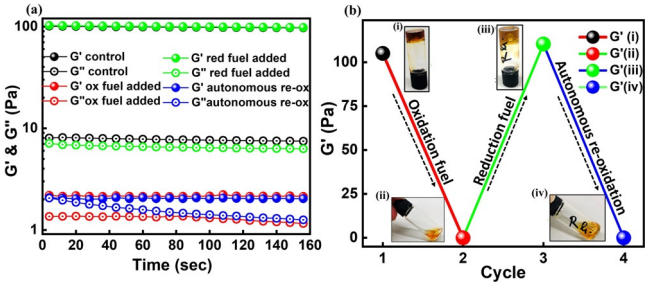

Figure 3. a) Time-dependent oscillatory rheological measurements of G′ and G″ at different phases of fuel addition. b) Conversion of hydrogel with addition of fuels with final attained G′ values. i, black data: control hydrogel with G′ = 110 Pa. ii, red data: addition of oxidation fuel to the hydrogel and measurement of G′ after 2 h, G′ dropped to 0.3 Pa. iii, green data: addition of reduction fuel to the sol and measurement of G′ after 7 h, the sol had converted back to gel as is clear from the snapshot of inverted vial test. The resultant G′ was 115 Pa. iv, blue data: the gel so formed changed to sol independently without addition of any fuel resulting in G′ dropping to 0.7 Pa.

oxidation catalyst as an increase in HRP from 0.3 mM to 0.5 mM decreased the transition time period by nearly 50% (SI Figure S9). Next, reduction catalyst GOx (0.3 mM) and fuel D-glucose (0.60 M) were added to the sol and stirred for nearly 5 min after which the stirring bar was removed and the gel was rested for ca 6 h. The reformed gels had similar storage modulus as the native ones, however the reassembled gels were not stable and changed into sol after ca 6 h of assembly without any addition of oxidation fuel (Figure 3b). This observation implies that the delayed negative feedback (re-oxidation) observed in the Fc solutions was also operating in the hydrogels. To make sure that the transformation into sol occurred due to oxidation of Fc, various control experiments were carried out including (i) addition of excess buffer (25 μL to 100 μL) to the gel and recording the resultant G′. It was found that G′ only changed from 100 Pa to 60 Pa but never converted to sol in the comparable time frames (SI Figure S10, methods (v)(iii)). (ii) Studies to determine minimum amount of oxidation fuel required for sol formation, such that there is no residual H_2O_2 present in the system (SI Figure S11, methods (v)(iv)). After establishing the above facts, in line with the UV/Vis studies carried out earlier, reduction experiments on sol with varying amounts of D-glucose at constant GOx concentration were carried out in order to modulate and control the negative feedback observed in the hydrogel. To analyze the sol-to-gel transitions, time-dependent rheology experiments were performed.

Briefly, to a freshly oxidized sol (containing HRP (0.3 mM) from prior oxidation) varying D-glucose concentrations (0.054 M to 0.96 M) and a constant amount of GOx (0.3 mM) were added. The resultant mixture was stirred at room temperature for 5 min and ca. 150 μL aliquot was transferred on to the rheometer. G′ and G″ were measured after fixed duration of 30 min for 15 h at room temperature (SI methods (iv)(c), Figure 4). All the samples were measured in triplicate. The rate of reduction and resultant degree of association of host–guest crosslinks in the gel were found to have a sinusoidal dependence on D-glucose concentration, that is, both reached a maximum and started to decrease with further increase in D-glucose concentration. Much like the trend observed for Fc, at lower concentration (0.054 and 0.16 M) of added D-glucose there appeared to be not enough D-glucose present, such that the rate of reduction was slow and the density of CD-Fc crosslinks reassembled was not high enough (G′ ≈ 60 and 80 Pa, respectively) to restore the native storage modulus G′ = 100 Pa. At 0.32 M of D-glucose added, a higher rate of reduction was observed, leading to the reassembly of an optimum density of crosslinks (G′ ≈ 100 Pa). However, the concentration of D-glucose was not yet high enough to initiate re-oxidation in the network. As the amount of D-glucose was further increased to 0.66 M we observed that although the initial rate of reduction had decreased, the final degree of crosslinking and the resultant G′ had increased to ≈ 130 Pa. This meant increased crosslinking and entanglement of the polymer chains as a result of annealing that rendered higher strength to the network, a phenomenon that is often observed in gel-sol-gel transitions.[12,38]

At 0.66 M D-glucose, an autonomous transformation of gel to sol is observed (in approx. 200 min) as the G′ dropped from

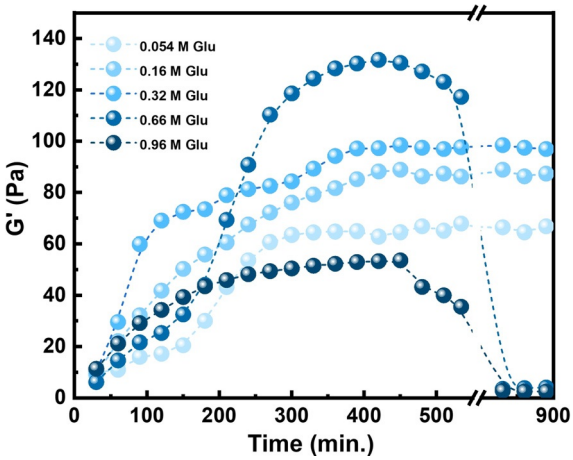

Figure 4. Time-dependent rheological measurements on oxidized sol with varying concentration of D-glucose. While at lower concentration of D-glucose (0.054, 0.16, 0.32 M) the samples converted from sol to gel and remained stable, at higher concentration of D-glucose (0.66, 0.96 M) an autonomous re-oxidation of gel to sol was observed.

130 Pa to mere 5.5 Pa towards the end of the experiment. This prompted us to further increase the concentration of D-glucose to 0.96 M, where we observed the slowest rate of reduction and the lowest degree of association (G′ ≈ 55 Pa), but as expected the higher concentration of D-glucose gave a 2–3 h faster transition to sol (G′ changed from 55 Pa to 4 Pa). The difference is likely due to an interplay of two factors arising in the network: (a) substrate inhibition effects due to very high concentration of D-glucose leading to formation of less GOx[$FADH_2$], which decreases the overall rate of reduction; (b) reduced diffusion in the hydrogel,[39] which limits the transfer of substrates and products to/from the enzymes. This disturbs the pre-organized chronological order of reactions in the hydrogel. As proposed above for Fc, the cofactor $FADH_2$ always prefers Fc^+ over dissolved O_2, maintaining the directionality of the reactions. However, due to the limited availability of $FADH_2$ in the reaction mixture combined with slower diffusion of Fc^+ and O_2, we observed competing reactions in the hydrogel.

To make sure that the sol formation observed at the end of the experiments in Figure 4 was due to reformation of oxidation fuel and not because of shear thinning of hydrogel in the course of the measurement, control experiments were performed by addition of chromophore substrate ABTS to the sol (SI Figure S12). There was an evident formation of $ABTS^{\bullet+}$ in the sol and the continuous absorbance measurements at 420 nm indicated an increase in the concentration of $ABTS^{\bullet+}$ over time, which meant that production of H_2O_2 was active for nearly 6 h as indicated by the UV/Vis studies. These observations indicate that both the time of negative feedback response and the strength of resultant hydrogel could be tuned by adjusting the concentration of only D-glucose in the network. Hence, although the host–guest polymer gel is typically a responsive supramolecular system that switches between two equilibrium states, the CRN showed emergence of a non-equilibrium state at high concentration of D-glucose.

Finally, the sequential selection of substrates by GOx-[$FADH_2$] (first Fc^+, then O_2) gave an opportunity to reprogram the gel to become self-regulating without exogenous injection of oxidation fuel H_2O_2 and disassemble autonomously in the presence of reduction fuel D-glucose. Thus, the hydrogel shows positive and negative feedback by adjusting its reaction with a non-redox substrate and switches autonomously from the gel to the sol state and back. This hypothesis was proved by addition of both enzymes HRP and GOx to the hydrogel and providing D-glucose to the system. Time-dependent rheological measurements were carried out to see if the gel changes to sol and eventually returns to the gel state (SI methods (iv)(d), Figure 5a).

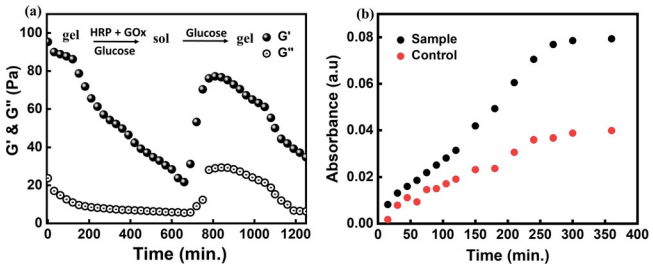

Figure 5. a) Time-dependent rheology shows self-regulating behavior of the supramolecular hydrogel in the presence of D-glucose. The measurement starts with a gel containing enzymes HRP and GOx with introduction of D-glucose. G′ and G″ were measured after every 30 min for 20 h. The gel first transformed into sol changing G′ from ca. 100 Pa to 23 Pa due to oxidation of Fc to Fc^+ over time. At this point, 0.66 M glucose was added again to run another cycle of gel-sol-gel transition. The sol returned to gel (Fc^+ reduced to Fc), which eventually transferred into sol (Fc oxidized to Fc^+) by a feedback in the network (autonomous production of H_2O_2) and showed a reversible transition between the two states with constant supply of D-glucose to the system. b) Carboxyfluorescein dye release showing sensitivity of hydrogel towards D-glucose (0.66 M) compared to a control hydrogel.

As can be observed from Figure 5a, the gel acted as a D-glucose sensor[40] and autonomously transformed from the gel to the sol state and vice versa, and only refueling the system with D-glucose (not H_2O_2) was required after every cycle. Large amounts of D-glucose could not be added in the beginning as it could lead to substrate inhibition as observed earlier. As a proof-of-concept, we used the D-glucose sensing ability of the gel for payload release. 0.8 mM carboxyfluorescein dye was added while mixing the two polymers (4 wt% pAA-CD and pAA-Fc) together with both the enzymes (0.3 mM each) HRP and GOx (SI methods (iii)(d), Figure 5b). It was seen that the amount of dye released was nearly twice as high for the gel incubated in the 0.66 M D-glucose solution compared to the control. Clearly, D-glucose can penetrate the dialysis membrane (MWCO 1 kDa) and interact with enzymes resulting in disassembling of glucose sensing hydrogel much faster than the control hydrogel. The formation of H_2O_2 in the sample gel was further supported by the fact that the absorption maximum for the sample was blue shifted to 452 and 476 nm rather than at 492 nm as observed for the control, which indicated oxidation[41] of dye in the presence of peroxide (SI Figure S13). This gave a clear indication that the gel could behave as a glucose sensor in solution and that H_2O_2 is generated leading to disassembly of the gel and a higher payload release.

Conclusion

We present a fuel-driven and enzyme-regulated supramolecular hydrogel that shows redox-response as well as emerging self-regulating behavior depending on the concentration of fuel (D-glucose) provided to the chemical reaction network. As a responsive network the hydrogel oscillates between two equilibrium states of gel and sol in response to the addition of oxidation fuel H_2O_2 and catalyst HRP or reduction fuel D-glucose and catalyst Gox. The enzyme–fuel couples act orthogonally to each other by initiating oxidation of Fc or reduction of Fc^+, respectively. At higher D-glucose concentrations, the enzyme-catalyzed reaction network generates the oxidation fuel H_2O_2. This negative feedback leads to a transition from the equilibrium responsive network into a non-equilibrium self-regulating network with autonomous assembly and disassembly of the hydrogel. Our results show that the kinetics of biocatalytic reaction networks can be orchestrated inside a hydrogel to design synthetic soft matter with self-regulating properties.

Acknowledgements

This work was funded by a CIM IMPRS Graduate School doctoral fellowship to MJ at the University of Münster. We are very grateful for inspiring discussions within the CRC 1459 “Intelligent Matter”. Open access funding enabled and organized by Projekt DEAL.

Conflict of Interest

The authors declare no conflict of interest.

Keywords: cyclodextrin · enzyme catalysis · hydrogels · non-equilibrium systems · self-regulating behavior

[1] a) J. H. van Esch, R. Klajn, S. Otto, *Chem. Soc. Rev.* **2017**, *46*, 5474 – 5475; b) X. He, M. Aizenberg, O. Kuksenok, L. D. Zarzar, A. Shastri, A. C. Balazs, J. Aizenberg, *Nature* **2012**, *487*, 214 – 218.

[2] a) J. Prost, F. Jülicher, J. F. Joanny, *Nat. Phys.* **2015**, *11*, 111 – 117; b) S. Banerjee, M. L. Gardel, U. S. Schwarz, *Annu. Rev. Condens. Matter Phys.* **2020**, *11*, 421 – 439.

[3] a) H. Hess, J. L. Ross, *Chem. Soc. Rev.* **2017**, *46*, 5570 – 5587; b) R. D. Astumian, *Faraday Discuss.* **2016**, *195*, 583 – 597; c) R. D. Astumian, *Nat. Commun.* **2019**, *10*, 3837.

[4] J. Howard, A. A. Hyman, in *Methods in Cell Biology, Vol. 39* (Ed.: J. M. Scholey), Academic Press, San Diego, **1993**, pp. 105 – 113.

[5] a) E. M. Mandelkow, G. Lange, A. Jagla, U. Spann, E. Mandelkow, *EMBO J.* **1988**, *7*, 357 – 365; b) T. Mitchison, M. Kirschner, *Nature* **1984**, *312*, 237 – 242.

[6] S. Inoue, S. Sugiyama, A. A. Travers, T. Ohyama, *Biochemistry* **2007**, *46*, 164 – 171.
[7] Z. Feng, T. Zhang, H. Wang, B. Xu, *Chem. Soc. Rev.* **2017**, *46*, 6470 – 6479.
[8] O. Valiron, N. Caudron, D. Job, *Cell. Mol. Life Sci.* **2001**, *58*, 2069 – 2084.
[9] a) A. Walther, *Adv. Mater.* **2020**, *32*, 1905111; b) M. M. Lerch, A. Grinthal, J. Aizenberg, *Adv. Mater.* **2020**, *32*, 1905554; c) S. N. Semenov, L. J. Kraft, A. Ainla, M. Zhao, M. Baghbanzadeh, V. E. Campbell, K. Kang, J. M. Fox, G. M. Whitesides, *Nature* **2016**, *537*, 656 – 660; d) J. Heckel, S. Loescher, R. T. Mathers, A. Walther, *Angew. Chem. Int. Ed.* **2021**, *60*, 7117 – 7125; *Angew. Chem.* **2021**, *133*, 7193 – 7201; e) C. Kaspar, B. J. Ravoo, W. G. van der Wiel, S. V. Wegner, W. H. P. Pernice, *Nature* **2021**, *594*, 345 – 355.
[10] J. Boekhoven, W. E. Hendriksen, G. J. M. Koper, R. Eelkema, J. H. van Esch, *Science* **2015**, *349*, 1075.
[11] a) S. Bal, K. Das, S. Ahmed, D. Das, *Angew. Chem. Int. Ed.* **2019**, *58*, 244 – 247; *Angew. Chem.* **2019**, *131*, 250 – 253; b) S. P. Afrose, S. Bal, A. Chatterjee, K. Das, D. Das, *Angew. Chem. Int. Ed.* **2019**, *58*, 15783 – 15787; *Angew. Chem.* **2019**, *131*, 15930 – 15934.
[12] N. Singh, B. Lainer, G. J. M. Formon, S. De Piccoli, T. M. Hermans, *J. Am. Chem. Soc.* **2020**, *142*, 4083 – 4087.
[13] a) T. Heuser, E. Weyandt, A. Walther, *Angew. Chem. Int. Ed.* **2015**, *54*, 13258 – 13262; *Angew. Chem.* **2015**, *127*, 13456 – 13460; b) J. Deng, A. Walther, *Nat. Commun.* **2020**, *11*, 3658.
[14] S. Dhiman, K. Jalani, S. J. George, *ACS Appl. Mater. Interfaces* **2020**, *12*, 5259 – 5264.
[15] X. Lang, U. Thumu, L. Yuan, C. Zheng, H. Zhang, L. He, H. Zhao, C. Zhao, *Chem. Commun.* **2021**, *57*, 5786 – 5789.
[16] A. Paul, R. Borrelli, H. Bouyanfif, S. Gottis, F. Sauvage, *ACS Omega* **2019**, *4*, 14780 – 14789.
[17] a) L. Tan, Y. Liu, W. Ha, L.-S. Ding, S.-L. Peng, S. Zhang, B.-J. Li, *Soft Matter* **2012**, *8*, 5746 – 5749; b) P. Du, J. Liu, G. Chen, M. Jiang, *Langmuir* **2011**, *27*, 9602 – 9608; c) B. V. K. J. Schmidt, C. Barner-Kowollik, *Angew. Chem. Int. Ed.* **2017**, *56*, 8350 – 8369; *Angew. Chem.* **2017**, *129*, 8468 – 8488.
[18] a) M. Ni, N. Zhang, W. Xia, X. Wu, C. Yao, X. Liu, X.-Y. Hu, C. Lin, L. Wang, *J. Am. Chem. Soc.* **2016**, *138*, 6643 – 6649; b) D. Astruc, *Eur. J. Inorg. Chem.* **2017**, 6 – 29; c) H.-Z. Bu, S. R. Mikkelsen, A. M. English, *Anal. Chem.* **1998**, *70*, 4320 – 4325; d) S. Wang, Z. Xu, T. Wang, T. Xiao, X.-Y. Hu, Y.-Z. Shen, L. Wang, *Nat. Commun.* **2018**, *9*, 1737; e) M. Inouye, M. Takase, *Angew. Chem. Int. Ed.* **2001**, *40*, 1746 – 1748; *Angew. Chem.* **2001**, *113*, 1796 – 1798; f) Y. Long, B. Song, C. Shi, W. Liu, H. Gu, *J. Appl. Polym. Sci.* **2020**, *137*, 48653.
[19] a) M. Nakahata, Y. Takashima, H. Yamaguchi, A. Harada, *Nat. Commun.* **2011**, *2*, 511; b) Y. Takashima, S. Hatanaka, M. Otsubo, M. Nakahata, T. Kakuta, A. Hashidzume, H. Yamaguchi, A. Harada, *Nat. Commun.* **2012**, *3*, 1270; c) H. Zhang, L. Peng, Y. Xin, Q. Yan, J. Y. Yuan, *Macromol. Symp.* **2013**, *329*, 66 – 69.
[20] a) E. J. Calvo, C. Danilowicz, L. Diaz, *J. Chem. Soc. Faraday Trans.* **1993**, *89*, 377 – 384; b) M. Zhang, C. C. Song, F. S. Du, Z. C. Li, *ACS Appl. Mater. Interfaces* **2017**, *9*, 25905 – 25914; c) Z. Yao, B. Zhang, T. Liang, J. Ding, Q. Min, J. J. Zhu, *ACS Appl. Mater. Interfaces* **2019**, *11*, 18995 – 19005; d) R. Ostafe, N. Fontaine, D. Frank, M. Ng Fuk Chong, R. Prodanovic, R. Pandjaitan, B. Offmann, F. Cadet, R. Fischer, *Biotechnol. Bioeng.* **2020**, *117*, 17 – 29; e) R. Matsumoto, M. Mochizuki, K. Kano, T. Ikeda, *Anal. Chem.* **2002**, *74*, 3297 – 3303; f) R. de laRica, R. M. Fratila, A. Szarpak, I. J. Huskens, A. H. Velders, *Angew. Chem. Int. Ed.* **2011**, *50*, 5704 – 5707; *Angew. Chem.* **2011**, *123*, 5822 – 5825.
[21] Y. S. Sohn, D. N. Hendrickson, H. B. Gray, *J. Am. Chem. Soc.* **1970**, *92*, 3233 – 3234.
[22] A. D. Ryabov, V. N. Goral, *J. Biol. Inorg. Chem.* **1997**, *2*, 182 – 190.
[23] D. N. Hendrickson, Y. S. Sohn, D. M. Duggan, H. B. Gray, *J. Chem. Phys.* **1973**, *58*, 4666 – 4675.
[24] P. M. Naveenkumar, S. Mann, K. P. Sharma, *Adv. Mater. Interfaces* **2019**, *6*, 1801593.
[25] G. Delaittre, I. C. Reynhout, J. J. L. M. Cornelissen, R. J. M. Nolte, *Chem. Eur. J.* **2009**, *15*, 12600 – 12603.
[26] M. Jain, R. G. Vaze, S. C. Ugrani, K. P. Sharma, *RSC Adv.* **2018**, *8*, 39029 – 39038.
[27] L. Zhu, R. Yang, J. Zhai, C. Tian, *Biosens. Bioelectron.* **2007**, *23*, 528 – 535.
[28] Y. Yong, P. Ouyang, J. Wu, Z. Liu, *ChemCatChem* **2020**, *12*, 528 – 535.
[29] S. Milker, M. J. Fink, N. Oberleitner, A. K. Ressmann, U. T. Bornscheuer, M. D. Mihovilovic, F. Rudroff, *ChemCatChem* **2017**, *9*, 3420 – 3427.
[30] A. M. Kunjapur, Y. Tarasova, K. L. J. Prather, *J. Am. Chem. Soc.* **2014**, *136*, 11644 – 11654.
[31] M. C. Hogan, J. M. Woodley, *Chem. Eng. Sci.* **2000**, *55*, 2001 – 2008.
[32] A. D. Ryabov, Y. N. Firsova, M. I. Nelen, *Appl. Biochem. Biotechnol.* **1996**, *61*, 25 – 37.
[33] a) J. Li, X. Li, Z. Zheng, X. Ding, *RSC Adv.* **2019**, *9*, 13168 – 13172; b) L. F. Salter, J. G. Sheppard, *Int. J. Chem. Kinet.* **1982**, *14*, 815 – 821.
[34] a) J. Mirón, M. P. González, J. A. Vázquez, L. Pastrana, M. A. Murado, *Enzyme Microb. Technol.* **2004**, *34*, 513 – 522; b) M. C. Reed, A. Lieb, H. F. Nijhout, *Bioessays* **2010**, *32*, 422 – 429.
[35] D. Petrović, D. Frank, S. C. L. Kamerlin, K. Hoffmann, B. Strodel, *ACS Catal.* **2017**, *7*, 6188 – 6197.
[36] R. Y. Zhang, E. Zaslavski, G. Vasilyev, M. Boas, E. Zussman, *Biomacromolecules* **2018**, *19*, 588 – 595.
[37] a) Y. Gao, Q. Luo, S. Qiao, L. Wang, Z. Dong, J. Xu, J. Liu, *Angew. Chem. Int. Ed.* **2014**, *53*, 9343 – 9346; *Angew. Chem.* **2014**, *126*, 9497 – 9500.
[38] Z. Cong, L. Zhang, L. Wang, J. Lin, *J. Chem. Phys.* **2016**, *144*, 114901.
[39] B. Amsden, *Macromolecules* **1998**, *31*, 8382 – 8395.
[40] H. R. Culver, J. R. Clegg, N. A. Peppas, *Acc. Chem. Res.* **2017**, *50*, 170 – 178.
[41] S. Pirillo, F. Sebastián García Einschlag, M. Luján Ferreira, E. H. Rueda, *J. Mol. Catal. B* **2010**, *66*, 63 – 71.

Manuscript received: June 14, 2021
Accepted manuscript online: July 12, 2021
Version of record online: August 11, 2021

